# Effects of conventional, extensive and semi-intensive green roofs on building conductive heat fluxes and surface temperatures in winter in Paris

Patrick Stella, Erwan Personne

# Effects of conventional, extensive and semi-intensive green roofs on building conductive heat fluxes and surface temperatures in winter in Paris

**P. Stella[1,*] and E. Personne[2]**

[1] Université Paris-Saclay, INRAE, AgroParisTech, UMR SADAPT, 75005, Paris, France

[2] Université Paris-Saclay, INRAE, AgroParisTech, UMR ECOSYS, 78850, Thiverval-Grignon, France

[*] Correspondence to: P. Stella (patrick.stella@agroparistech.fr)

**Highlights**

- Conventional, extensive and semi-intensive green roofs have been compared.
- Green roofs reduced temperature and heat flux fluctuations at the building surface.
- Deeper substrates reduced the temperature and heat flux fluctuations of the building surface.
- On average there was no or only slight effects on winter surface urban heat island.

**Abstract**

This study investigated the impacts of extensive and semi-intensive green roofs on both building insulation and surface urban heat island effect under winter conditions. To this aim we compared measurements of surface and building envelope temperatures as well as conductive heat fluxes reaching the external building envelope with those measured on a conventional bituminous roof under identical climatic conditions. The main effect of green roofs was to decrease daily fluctuations of external building envelope temperatures and as a consequence to reduce fluctuations of conductive heat fluxes reaching the building envelope. This effect is all the more important that the substrate is deep, in link with its heat capacity and thermal inertia.

Yet, no significant effect of the green roofs on surface urban heat island has been observed on average despite a surface cooling during daytime. It is concluded that the green roofs can be suitable urban greening solutions since they do not have negative effect on surface urban heat island during winter, provide cooling during summer, and contribute to building insulation inducing therefore building energy savings.

**Keywords**

Green roofs; building insulation; urban heat island; conductive heat fluxes; winter conditions.

## 1 – INTRODUCTION

Urban areas and land-use changes lead to severe environmental issues due to urbanization. On the one hand, urban areas are strong contributors to greenhouse gas (GHG) emissions at the global scale and therefore to global warming. It is estimated that buildings are responsible for 19% of all global 2010 energy-related GHG emissions, mainly indirect ones from electricity use. Yet, buildings account for 32% of total global final energy use, space heating and cooling representing more than one third of total building final energy consumption [1]. On the other hand, at the local scale the land-use modifications due to urbanization alter the urban microclimate and induce the so-called "urban heat island" (UHI) effect [2,3] which reflects the fact that cities are warmer than their surroundings. It has numerous impacts on building energy consumption (e.g., [4-5]), citizen comfort and health (e.g., [6-8]), and urban air quality (e.g., [4, 9-10]). This phenomenon originates from the alteration of radiative budget and energy balance, in which the heat released by anthropogenic activities is a strong contributor to UHI effect. Indeed, anthropogenic heat release occurs mainly through building cooling and heating (e.g., [11]) and is responsible for an increase in urban air temperatures between 0.2 and 2.5°C (e.g., [12,13]). Within this context, the building insulation assessment allows (i) to mitigate UHI effect (through the decrease of anthropogenic heat release) and its related deleterious effects at the local scale, (ii) subsequent monetary savings, and (iii) to reduce the GHG emissions at the global scale [1].

Among the numerous techniques to improve building insulation (e.g., insulation layer depth, new insulation materials) (e.g., [14-17]), green roofs currently receive strong attention. Additionally to building insulation, they contribute to the assessment of urban air quality (e.g., [18,19]), the water retention to prevent runoff events (e.g., [19-21]), sound reduction and insulation, ecological preservation (e.g., [21,22]), and last but not least direct UHI mitigation owing to their capability to refresh air throughout evapotranspiration (e.g., [23,24]).

Green roofs i.e., vegetated systems covering a building rooftop, are typically composed by some layers aiming to protect the building envelope (i.e., waterproofing membrane, root barrier, drainage layer), a growing medium (or substrate) layer, and a vegetation layer. It is distinguished the extensive, semi-intensive, and intensive green roofs, each characterized by the substrate thickness and plant communities [25]. Owing to plant shading, evaporative cooling, and additional insulation, green roofs help to reduce directly building energy consumption but also indirectly through UHI mitigation. However, the thermal performance of green roofs is highly variable according to the substrate and vegetation characteristics, building characteristics, and local climatic conditions. (e.g., [26-30]).

Many studies focused their attention on the impacts of green roofs on building insulation and building thermal performance, as well as on UHI mitigation, under summer conditions (e.g., [24, 28, 31-35]). Overall, it is consensual that green roofs reduce surface and air temperatures, diminish heat fluxes entering inside the building, and therefore decrease energy consumption for cooling. However, the impact of green roofs under winter conditions received less attention, and is still under debate. For instance, Santamouris et al. [36] did not found any significant effect of green roof on heating load variation under winter Mediterranean climate, while Jaffal et al. [28] reported positive impact of extensive green roofs under temperate oceanic climatic conditions. Yet, during heating period, Coma et al. [37] reported a negative impact of extensive green roof on building energy consumption under continental climate conditions, whereas under similar climatic conditions Lundholm et al. [38] found lower net heat losses from extensive green compared to conventional roofs. Moreover, experimental studies carried out under winter conditions mainly considered only one kind of green roofs, often extensive ones [37-46], without comparing the extensive, semi-intensive, and intensive green roofs together. Last, considering that winter UHI would be positive concerning building energy consumption, in particular by reducing the indoor and outdoor temperature difference, surface (and

consequently air) cooling by green roofs would be deleterious. This issue has not been explored yet.

The objectives of this study are (i) to analyze how green roofs affect winter thermal fluxes reaching the building envelope, (ii) to determine their impact on winter surface UHI, and (iii) to compare extensive and semi-intensive green roofs under winter oceanic climatic conditions, from an experimental approach.

## 2 – MATERIALS AND METHODS

### 2.1 – Site description

The experiment was carried out from 1st November 2018 to 28th January 2019 in Paris, France. The climate is oceanic and characterized by overall cool winter. The experiment was performed on the building rooftop of AgroParisTech, higher education and research institute located in the 5th district of Paris (48°50'24"N, 2°20'55"E). It is a Haussmannian building built during the 19th century. The rooftop area is about 900 $m^2$ and is exposed to direct solar radiation without shadowing effect from other buildings. The indoor spaces consisted in office rooms. Since the indoor uses are similar for the three roofs, the indoor conditions (especially indoor temperatures) did not differ between each roofs. The heating system only consisted in individual heater alimented by a common boiler, and no central temperature heating regulating system existed.

The experiment was performed on three different areas: the reference roof (REF) and the extensive (EXT) and semi-intensive (SI) green roofs. The reference is a conventional roof with a black bituminous waterproof membrane installed directly on the concrete slab. The green roofs are installed directly on the bituminous waterproof membrane and consisted in a root barrier, a substrate layer (13 cm for EXT, 27 cm for SI), and a vegetation layer (sparse Sedum

for EXT; dense grass for SI) (Figure 1). For the EXT green roof, plant coverage accounted for 22% while it was close to 100% for the SI green roof.

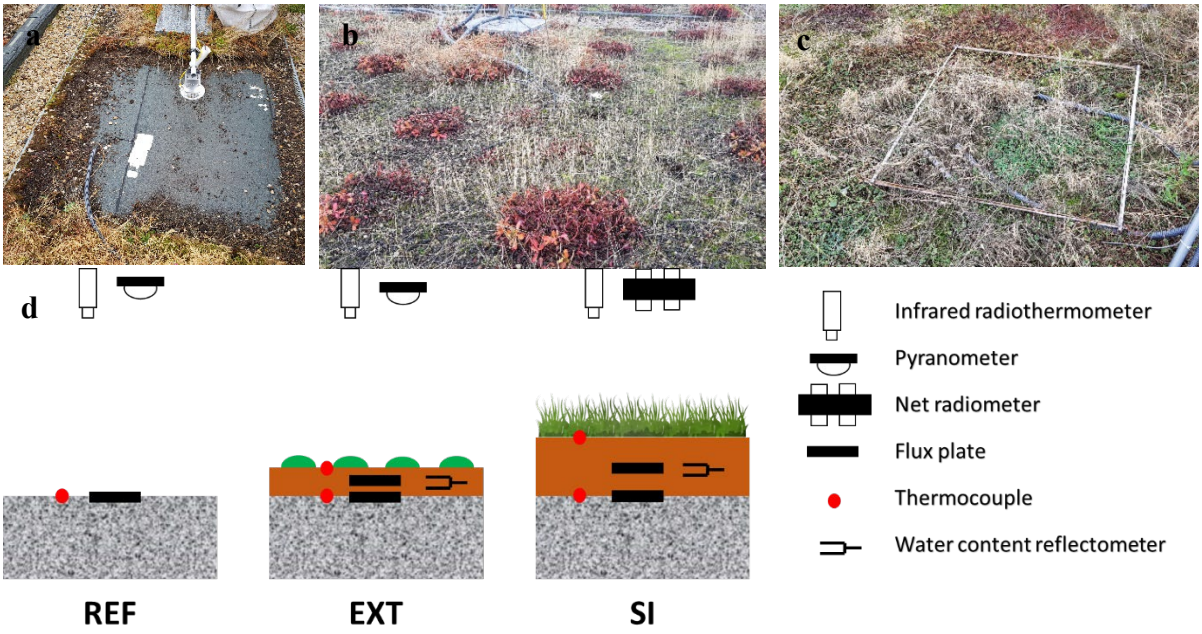


**Figure 1: (a)** The reference roof and vegetation covering the **(b)** extensive and **(c)** semi-intensive green roofs. **(d)** Scheme of the experimental set-up and measurements on the conventional (REF), extensive (EXT) and semi-intensive (SI) green roofs.

## 2.2 – Instrumentation and measurements

For each roof, the mean surface temperature was measured by an infrared radiothermometer (IR120, Campbell Scientific Ltd, UK) installed on a mast at 1.05 m height above the REF roof and 2 m height above EXT and SI green roofs. The surface measured by the sensor (half-angle of view of 20°) was therefore 0.4 $m^2$ for the REF roof and 1.6 $m^2$ for the EXT and SI green roofs. Additionally, each component of the radiative budget (i.e., incoming and outgoing short- and longwave radiations) were measured with a net radiometer (CNR4, Kipp & Zonen, NL) above the SI green roof, while only the outgoing (i.e., reflected) shortwave radiation was measured with a pyranometer (CMP11, Kipp & Zonen, NL) above the REF and EXT roofs. Moreover, five thermocouples (Type T, TC Direct, FR) were installed to provide temperature measurements: on the black bituminous membrane for the REF roof and on the substrate and at

125 the substrate-building envelope interface for both green roofs. Conductive heat fluxes inside
126 the substrate (installed at 6.5 cm and 13 cm depth for EXT and SI green roofs, respectively)
127 and outside the building envelope (i.e., installed directly on the bituminous membrane for the
128 REF roof and at the substrate-building envelope interface for both green roofs) were also
129 measured by heat flux plates (HFP01, Hukseflux, NL). Finally, water content reflectometers
130 (CS655, Campbell Scientific Ltd, UK), installed at 6.5 cm and 13 cm depth for EXT and SI
131 green roofs, respectively, provided measurements of volumetric substrate water content (Figure
132 1d). All the sensors were connected to a datalogger (CR1000X, Campbell Scientific Ltd, UK)
133 coupled with two multiplexers (AM16/32, Campbell Scientific Ltd, UK). Measurements were
134 averaged online over 30 min periods.
135 Additionally, standard meteorological conditions were measured at 2.5 m height above the roof
136 by several sensors installed on a mast located on the roof at around 50 m from the experimental
137 area: air temperature and relative humidity (HMP45C, Vaisala, FI), and rainfall (TE525WS,
138 Campbell Scientific Ltd, UK). They were measured, averaged, and recorded every 30 min on a
139 datalogger (CR1000, Campbell Scientific Ltd, UK).
140 The ranges and accuracies of the sensors used during the experiment are given Table 1.
141
142 **Table 1:** List of sensors, their range and accuracy used during the experiment

| Measured variable | Sensor | Range | Accuracy |
|---|---|---|---|
| Mean surface temperature | Infrared radiothermometer IR120 | -25 to +60°C | ±0.2°C |
| Temperature | Thermocouple Type T | -50 to +150°C | ±0.1°C |
| Air temperature and relative humidity | Thermo-hygrometer HMP45C | -39 to +60°C<br>0.8 to 100% | ±0.2°C<br>±1% |
| Shortwave radiation | Net radiometer CNR4<br>Pyranometer CMP11 | 0 to 2000 W.m$^2$<br>0 to 4000 W.m$^2$ | ±10%<br><2% |
| Longwave radiation | Net radiometer CNR4 | [-] | <10% |
| Conductive heat flux | Heat flux plate HFP01 | ±2000 W.m$^{-2}$ | -15 to +5% according to the material in contact |
| Substrate water content | Reflectometer CS655 | 0 to 100% | ±3% |

| | | | |
|---|---|---|---|
| Rainfall | Rain gauge TE525WS | [-] | -3.5 to +1% according the intensity of rainfall |

## 3 – RESULTS AND DISCUSSION

### 3.1 – Overview of weather conditions

During our experiment, weather conditions were representative of the winter climate in Paris. Both daily and day-to-day variability of the weather conditions are reported through the half-hourly and daily statistics, respectively, in Figure 2 and Table 2. The cumulated solar radiation over the experimental period was 257 $MJ.m^{-2}$ over the 83 days of the experiment (Table 2). The incident solar radiation followed a typical trend by increasing during the morning to reach its maximum at noon, on average around 150 $W.m^{-2}$, before decreasing during the afternoon to its minimum and nocturnal value at 0 $W.m^{-2}$ (Figure 2a). Its intensity was weak: half-hourly solar radiation was 145 ± 88 $W.m^{-2}$ on average and varied overall between 75 $W.m^{-2}$ and 198 $W.m^{-2}$, as indicated by the 1st and 3rd quartiles respectively. However, some sunny days occurred, as indicated by the maximum half-hourly solar radiation (520 $W.m^{-2}$). At the daily scale, mean solar radiation was only 127 ± 61 $W.m^{-2}$ and daily mean solar intensity usually ranged between 78 $W.m^{-2}$ and 183 $W.m^{-2}$ with a minimum and maximum at 51 $W.m^{-2}$ and 256 $W.m^{-2}$, respectively (Table 2). Air temperature and relative humidity exhibited an inverse correlation. Air temperature increased from its minimum, on average 6.3°C just before the sunrise, to its maximum in early afternoon, on average 8.7°C, and then decreased progressively during the afternoon and the night. Conversely, air relative humidity decreased from its maximum at the sunrise, around 87% on average, to its minimum, around 77% on average, reached in early afternoon, and finally increased in the afternoon and during nighttime (Figure 2b). Few particularly dry and warm days for the season occurred with maximum half-hourly and daily mean temperatures of 19.5°C and 15.3°C, respectively, and minimum half-hourly and daily mean air relative humidity of 40% and 65%, respectively. Some cold events also occurred, with

167 negative minimum half-hourly and mean daily air temperatures. Overall, climatic conditions
168 were cold and wet as indicated by mean and median values, around 7.4-7.8°C and 84-86% for
169 air temperature and relative humidity respectively, both at the half-hourly and daily scales.
170 (Table 2). Yet, rainfall events regularly occurred: 51 days with at least one rainfall event were
171 recorded corresponding to 337 half-hourly events over the whole experimental period. On
172 average, rainfall events were 0.46 mm and 3.02 mm at the half-hourly and daily scales,
173 respectively, but some exceptional and strong episodes appeared, 2.6 mm at the half-hourly
174 scale and 14.2 mm at the daily scale on maximum. Over the three months of the experiment the
175 cumulated rainfall was 154.2 mm (Table 2). As a consequence, green roof did not suffer from
176 water limitation, mean substrate water content (0.29 $m^3.m^{-3}$ and 0.14 $m^3.m^{-3}$ for EXT and SI
177 green roofs, respectively) being close to their maximum (0.46 $m^3.m^{-3}$ and 0.19 $m^3.m^{-3}$ EXT and
178 SI green roofs, respectively). Yet, the regular rainfall events allowed a quite stable substrate
179 water content over the period for both EXT and SI green roofs, as indicated by the weak range
180 of variations between 1$^{st}$ and 3$^{rd}$ quartiles of the substrate water contents (0.25 to 0.32 for EXT
181 green roof; 0.13 to 0.16 for SI green roof) (Table 2). As a consequence, the effect of soil water
182 content variations on temperatures and conductive heat fluxes could be excluded.

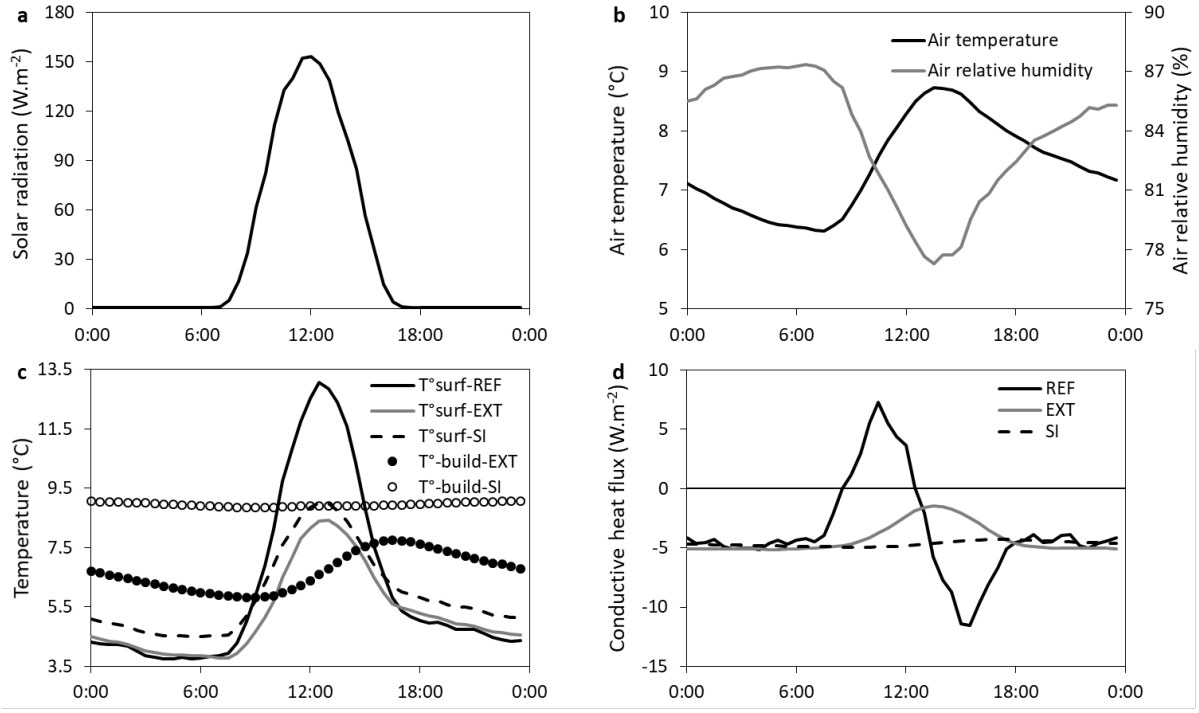


**Figure 2:** Half hourly means of **(a)** solar radiation, **(b)** air temperature (black line) and relative humidity (grey line), **(c)** surface temperatures of the reference (T°-surf-REF; black line), extensive (T°-surf-EXT; grey line), and semi-intensive (T°-surf-SI; dashed black line) roofs, and temperatures at the substrate-building envelope interface for extensive (T°-build-EXT; filled circles) and semi-intensive (T°build-SI; open circles) green roofs, and **(d)** conductive heat flux outside the building envelope for the reference (REF; black line), extensive (EXT; grey line), and semi-intensive (SI; dashed black line).

**Table 2:** Half-hourly and daily means (± standard deviations), medians, minimums, maximums, and 1st and 3rd quartiles of solar radiation, air temperature, air relative humidity, rainfall events, and substrate water content for extensive and intensive green roofs. The number of rainfall events (n) and cumulated rainfall over the experimental period are also given

| | | Solar radiation $W.m^{-2}$ | Air temperature °C | Air relative humidity % | Rainfall events mm | Substrate water content $m^3.m^{-3}$ | |
|---|---|---|---|---|---|---|---|
| | | | | | | Extensive | Semi-intensive |
| Half-hourly | Mean ± SD | 145±88 | 7.4±3.9 | 84±10 | 0.46±0.37 | 0.29±0.03 | 0.14±0.03 |
| | Min | 0 | -2.4 | 40 | 0.2 | 0.15 | 0.03 |
| | 1st quartile | 75 | 4.8 | 77 | 0.2 | 0.25 | 0.13 |
| | Median | 115 | 7.7 | 86 | 0.2 | 0.29 | 0.15 |
| | 3rd quartile | 198 | 10.3 | 92 | 0.6 | 0.32 | 0.16 |
| | Max | 520 | 19.5 | 99 | 2.6 | 0.46 | 0.19 |
| | n | - | - | - | 337 | - | - |
| Daily | Mean ± SD | 127±61 | 7.4±3.7 | 84±8 | 3.02±3.20 | 0.29±0.06 | 0.14±0.03 |
| | Min | 51 | -0.3 | 65 | 0.2 | 0.16 | 0.03 |
| | 1st quartile | 78 | 4.9 | 79 | 0.8 | 0.25 | 0.13 |
| | Median | 106 | 7.8 | 84 | 2.0 | 0.28 | 0.15 |
| | 3rd quartile | 183 | 10.2 | 90 | 4.2 | 0.33 | 0.16 |
| | Max | 256 | 15.3 | 97 | 14.2 | 0.43 | 0.17 |
| | n | - | - | - | 51 | - | - |
| Whole period | Sum | 257 $MJ.m^{-2}$ | - | - | 154.2 | - | - |

### 3.2 – Albedo values of conventional and green roofs

The albedos for conventional and green roofs were determined by linear regressions between the measured incident and reflected shortwave solar radiations, albedos being given by the slopes of the regression lines. The SI green roof exhibited the largest albedo (0.16) while the EXT green roof had the weakest one (0.12). The REF roof showed an intermediate albedo (0.15) but also the most variable as indicated by the coefficient of determination of the relationships ($R^2$ = 0.82). Albedo variability was the weakest for the SI green roof ($R^2$ = 0.95) and intermediate for EXT green roof ($R^2$ = 0.90) (Figure 3).

Whereas Radhi et al. [47] reported largest albedo (0.23) for bituminous membrane, the albedo for the REF roof determined experimentally is consistent with the typical range, 0.1-0.2, found for bitumen roofs [48]. For the green roofs, although previous studies did not distinguished between their different kinds i.e., extensive, semi-intensive or intensive, Lazzarin et al. [39] reported green roof albedo of 0.23 and Takebayashi and Moriyama [49] determined soil and grass albedos of 0.225 and 0.21, respectively, for dry surface conditions. The albedos for EXT and SI green roofs are lower than these studies, but consistent with the results obtained by D'Orazio et al. [42] who measured green roof albedo of 0.13. On the one hand, these weak albedos for green roofs compared to those reported in previous studies can be explained first by the season of the experiment. While previous studies were carried out under spring and summer conditions implying green and fully developed canopy cover, the winter season implies brown and less developed vegetation. It induces that the vegetation albedo is lower, and the soil (typically a dark material) albedo contributes more to total green roof albedo. It also probably explains the lowest albedo for the EXT green roof than for the SI green roof: since vegetation is sparser, the lower soil albedo contributes more to the total EXT green roof albedo than for the SI green roof. On the other hand, wetter conditions during winter than during spring and summer induces darker color of the soil surface and bituminous membrane leading to lower albedos. This issue could also explain the large variability of albedo for the REF roof and EXT green roof which would reflect the wetting and drying of the surface alternately during the experiment.

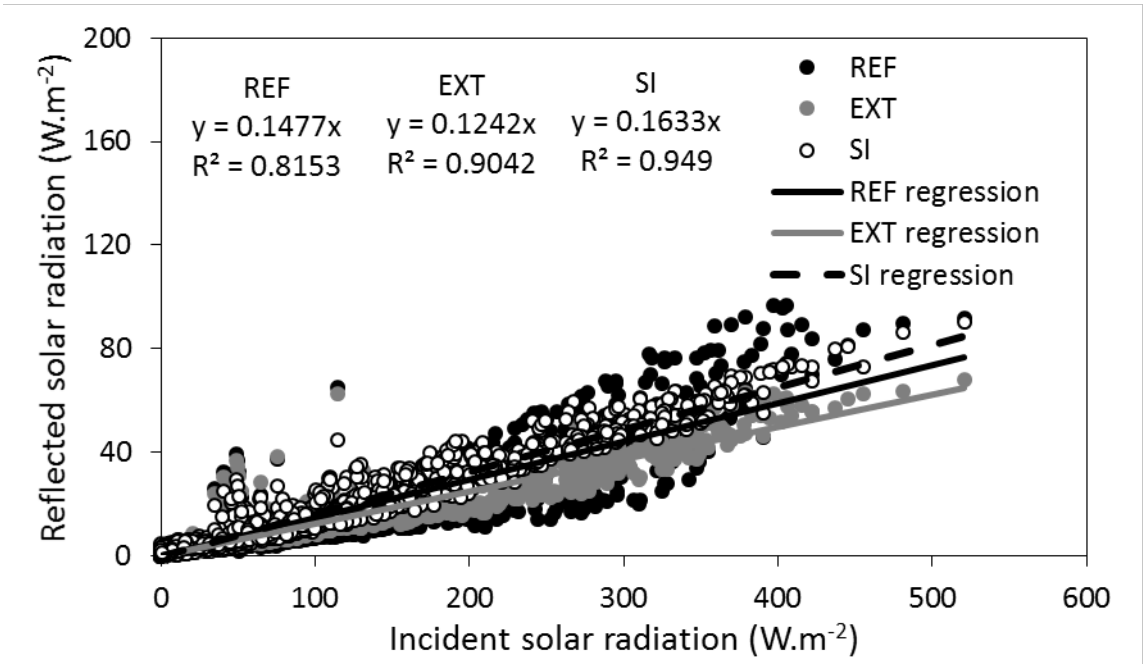


225

226 **Figure 3:** Relationships between incident and reflected solar radiation for the reference (REF;
227 black symbols), extensive (EXT; grey symbols), and semi-intensive (SI; open symbols) roofs.
228 Black, grey, and dashed black lines are regressions for REF, EXT, and SI roofs, respectively.

229

230 **3.3 – Impact of green roofs on building insulation**

231 In order to evaluate the impact of the green roofs on building insulation, temperatures and
232 conductive heat fluxes at the building surface (corresponding to surface temperature for the
233 REF roof and temperature at the substrate-building envelope interface for green roofs) have
234 been analyzed and compared between REF, EXT and SI roofs.

235 For the REF roof, the building surface temperature exhibited the largest fluctuation and
236 followed the dynamic of solar radiation by increasing during the morning to reach its maximum
237 around noon, on average around 13°C, before decreasing during the afternoon to its minimum
238 and nocturnal value at 3.5-5°C (Figure 2c). Over the whole experimental period median
239 building surface temperature was 6.4°C, typically ranged from 2.6°C to 9.5°C (1$^{st}$ and 3$^{rd}$
240 quartiles), and up to -7.2 to 19.8 for the minimum and maximum values (Figure 4a). The
241 conductive heat fluxes reaching the building envelope strongly varied across the day. During

242 nighttime, mean half hourly fluxes were negative indicating heat losses from the building,
243 around -5 $W.m^{-2}$. It increased from sunrise to reach its maximum (around 7 $W.m^{-2}$) in late
244 morning, and decreased until middle afternoon to its minimum (-11 $W.m^{-2}$). Finally it increased
245 until sunset to reach its nocturnal value. The building therefore lost heat most of the time,
246 excepted during a short period during the morning for which building gained heat as indicated
247 by the positive values (Figure 2d).
248 Considering only the whole period the EXT green roof exhibited similar median building
249 surface temperature (7°C) and 1st and 3rd quartiles (3.6°C and 9.4°C, respectively) to those
250 observed for the REF roof (Figure 4a). However building surface temperature for EXT green
251 roof exhibited less fluctuations than REF roof as indicated by both their minimum and
252 maximum values (0.4°C and 15.7°C, respectively; Figure 4a) and its daily pattern (Figure 2c).
253 Indeed the minimal mean half hourly building surface temperature was 6°C and occurred only
254 in late morning. It reached its maximum, around 8°C, in late afternoon and continuously
255 decreased during nighttime (Figure 2c). Hence, the building surface for EXT green roof was
256 warmer than for REF roof most of the time, excepted between 9:00 and 15:00 for which it was
257 cooler (Figure 2c). The temperature difference between REF and EXT roofs typically ranged
258 between -3.1°C (1st quartile) and 1.2°C (3rd quartile), overall at -0.8°C (median) indicating that
259 the building surface was slightly warmer for the EXT green roof than for the REF roof.
260 However, the building surface for the EXT green roof could be warmer (typically during
261 nighttime) or cooler (typically during daytime) by several degrees as indicated by the minimum
262 (-9.8°C) and maximum (7.7°C) values of the temperature difference (Figure 4b). On average
263 over the whole period, the conductive heat fluxes reaching the building envelope were always
264 negative, indicating heat losses from the building. However, they exhibited less diurnal
265 fluctuations than for the REF roof. The mean half hourly conductive heat flux was -5 $W.m^{-2}$

during nighttime, increased during the morning to peak at -1.5 $W.m^{-2}$ in early afternoon, and decreased to its nighttime value during the afternoon (Figure 2d).

The mean half hourly conductive heat fluxes reaching the building envelope and building surface temperatures for the SI green roof did not exhibited diurnal fluctuations: the former remained at around -4.5 $W.m^{-2}$ and the latter at around 9°C (Figures 2d and 2c, respectively). The building surface temperature exhibited also less fluctuation as shown by the 1st and 3rd quartiles (6.9°C and 11.4°C, respectively) and minimum and maximum (3.1°C and 14.2°C, respectively) temperatures (Figure 4a). Over the whole period the SI green roof also exhibited the warmest building surface envelope with a median temperature of 8.9°C (Figure 4a). The building surface for the SI green roof was most of the time warmer than for the REF roof: the temperature difference over the whole period was -2.6°C (median), typically varied between -0.2°C to -5.4°C (1st and 3rd quartiles), and could reach -14.1°C (minimum). However, it could also be cooler than for the REF roof, although it remained exceptional and typically during daytime, as indicated by the maximum value of the building enveloped temperature difference reaching 7.6°C (Figure 4b).

Hence, huge differences has been observed concerning the impact of the green roofs on the conductive heat fluxes reaching the building envelope. Nevertheless, these fluxes are also closely linked with indoor temperatures, depending themselves to building users. In this study, indoor environments consisted in offices and it has been hypothesis that indoor temperatures were identical for each green roofs. However, since office users could control the room heating, some differences could occur between indoors temperatures. The conductive heat flux (G) depends on the building envelope surface temperature difference between outdoor and indoor ($T_{out}$ and $T_{in}$, respectively) and on the thermal transmittance ($U_{value}$ in $W.m^{-2}.K^{-1}$) (i.e., $G = U_{value} \times (T_{out} - T_{in})$). Considering a $U_{value}$ of 3.33 $W.m^{-2}.K^{-1}$ (reported by Fokaides and Kalogirou [50] for a flat and non-insulated roof made of reinforced concrete, which is comparable to the studied

building), a change of 1°C of the indoor building surface envelope would lead to a change of 3.33 $W.m^{-2}$ of the conductive heat flux reaching the external building envelope, which would not affect the trends observed during the experiment. In addition, the nocturnal conductive heat fluxes similar for each roofs (Figure 2d), corresponding to heat losses from the building, suggested that the indoor temperatures were identical for REF, EXT, and SI roofs.

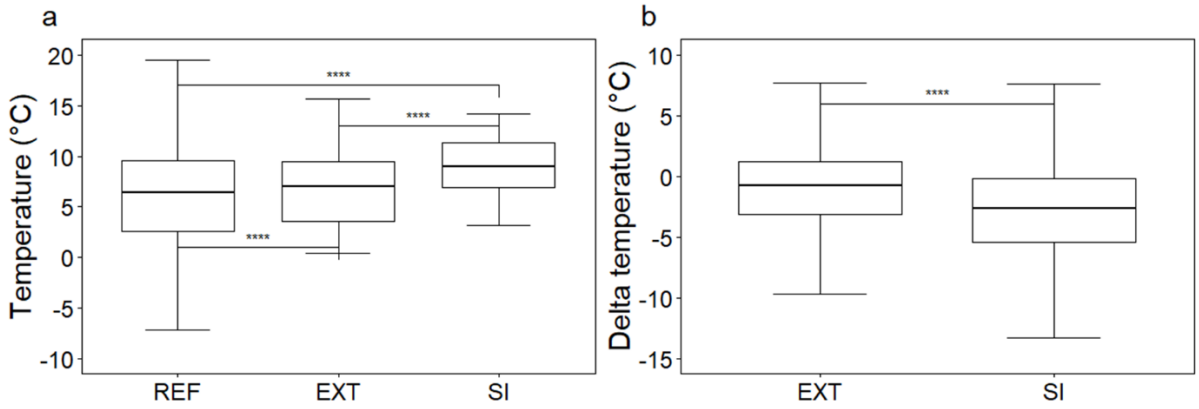


**Figure 4:** Boxplot statistics of **(a)** surface temperatures of the reference (REF) roof and temperatures at the substrate-building envelope interface for the extensive (EXT) and semi-intensive (SI) roofs, and **(b)** half-hourly differences between surface temperature of the reference roof and temperature at the substrate-building envelope interface for the green roofs. Are also indicated the results from the Wilcoxon statistical test (**** = p-value < 0.0001).

Although they were only interested in EXT green roofs during winter conditions, previous studies also found that the green roofs exhibited weak fluctuations of the building surface envelope temperatures under Mediterranean [37] and continental [45] climates, and less than for the conventional roofs. For instance Teemusk and Mander [40] reported during the winter period for continental climate monthly variation of daily temperature amplitudes between around 1°C and 2.5°C approximately for a green roof while they reached up to 5°C for the conventional roof. Similarly Getter et al. [41] reported for a Midwestern U.S. climate building envelope temperature varying between -4°C during nighttime and 10°C during daytime for a

311 conventional roof whereas it only ranged from around -1°C to 2°C for the green roof. These
312 largest temperature fluctuations for the conventional roof are linked with the absence of
313 substrate and vegetation layer, allowing a direct exposure of the building envelope to solar
314 radiation. It induces that the building envelope for the conventional roof rapidly warms during
315 daytime due to the fast increase of incident radiation, but also cools faster due to fast radiative
316 losses. On the contrary, the building envelope with a green roof is not directly exposed to the
317 solar radiation. The energy received at the green roof surface needs to be transferred through
318 the conductive heat flux within the substrate which is less efficient than the direct exposure to
319 sun radiation. This issue explains that the maximum building envelope temperature for the EXT
320 green roof only occurred in late afternoon while it occurred around noon for the REF roof. Yet,
321 the green roof substrate also prevents direct building envelope cooling from radiative losses.
322 The presence of substrate is therefore of a key importance for the assessment of building
323 insulation during winter, and its thickness the main factor controlling its efficiency since
324 vegetation is sparse and weakly evapotranspirates under such conditions, whatever the kind of
325 green roof (i.e., EXT or SI) considered. Indeed, the grass transpiration under winter conditions
326 only accounts for a small part of the total evapotranspiration, between 5-20% [51]. Hence,
327 although the vegetation densities are quite different between EXT and SI green roofs (with a
328 percentage of plant cover of approximatively 20-25% for EXT and 100% for SI, which is partly
329 composed of yellow and inactive leaves), it could be expected that the total evapotranspiration
330 is mainly driven by soil evaporation during winter conditions, which depends on atmospheric
331 conditions (identical for the two roofs) and substrate water content (always close to the field
332 capacity during the experiment). That would lead to a similar evapotranspiration for EXT and
333 SI green roof under winter condition despite the differences in terms of LAI and canopy cover,
334 as confirmed by Silva et al. [44].

As illustrated in Figure 5 the conductive heat fluxes within the substrate varied between -20 $W.m^{-2}$ and 35 $W.m^{-2}$ for the EXT green roof (Figure 5a) while it only ranged from -10 $W.m^{-2}$ to 5 $W.m^{-2}$ for the SI green roof (Figure 5b) for the same period from 2 November to 17 November 2018. This trend is probably due to heat storage within the substrate which is all the more important that the substrate is deep. Yet it is observed a time lag between (i) the temperature difference between substrate surface and substrate-building envelope interface and (ii) the conductive heat flux within the substrate for the SI green roof (Figure 5b), which did not occurred for the EXT green roof (Figure 5a). Hence the thick substrate of the SI green roof provides large thermal inertia. As a consequence the conductive heat fluxes reaching the building envelope exhibit less fluctuation with than without a green roof, and this effect increases with the substrate thickness. That issue was also found by D'Orazio et al. [42] who compared EXT green roof with conventional ones.

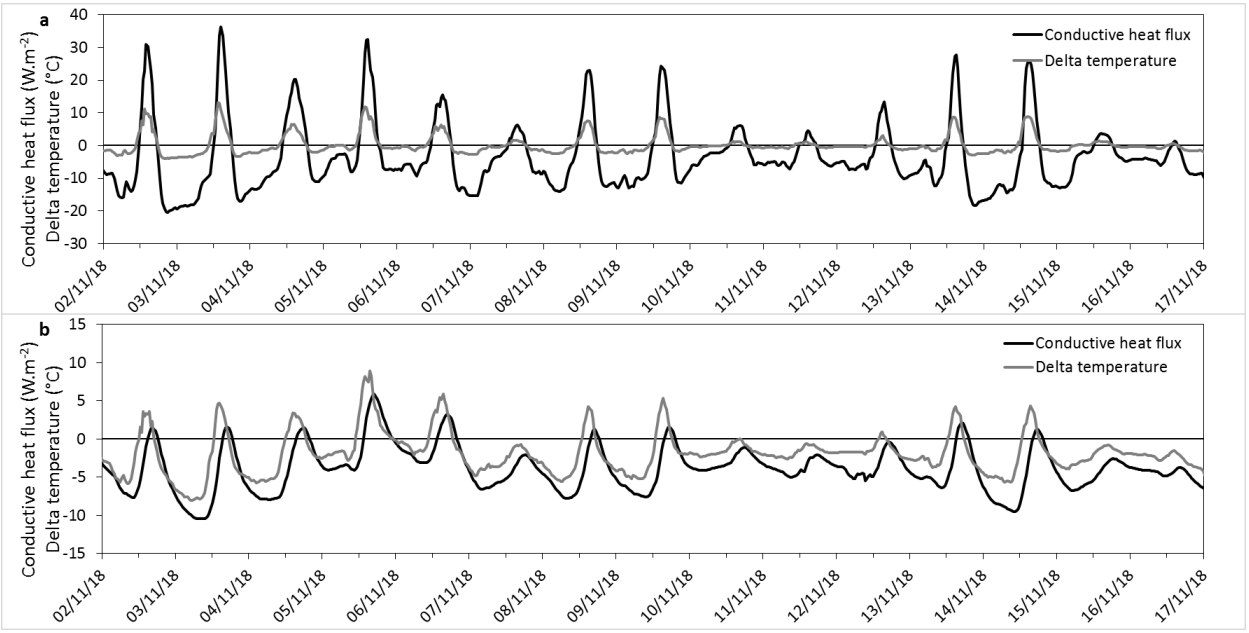


**Figure 5:** Time series of half-hourly conductive heat fluxes within the substrate and temperature differences between the substrate surface and the substrate-building envelope interface for the **(a)** extensive and **(b)** semi-intensive green roofs.

### 3.4 – Impact of green roofs on winter surface urban heat island

The impact of the green roofs on winter surface UHI has been explored by comparing the surface temperatures for the REF, EXT, and SI roofs. The surface temperatures for the REF roof are those presented in the previous section and will not be described in this section.

Considering the whole period the EXT green roof had median surface temperature of 5.6°C (2°C and 8.4°C for the 1st and 3rd quartiles, respectively), minimum and maximum surface temperatures reaching -3.9°C and 18.2°C, respectively. The SI green roof had slightly warmer surface temperature with median value equal to 6.2°C and 1st and 3rd quartiles of 3°C and 8.9°C, respectively. The minimum and maximum surface temperature were similar than for the EXT green roof. Considering the whole period, the surface temperature of the SI green roof did not differ significantly to the surface temperature of the REF roof while the EXT green roof is cooler, as indicated by the results of the Wilcoxon statistical tests (Figure 6a). Indeed, the half-hourly difference between surface temperatures of the REF and SI roofs typically ranged between -1.1°C and 0.9°C (1st and 3rd quartiles) with a median value of 0.2°C whereas this difference varied between -0.5°C and 1.6°C (1st and 3rd quartiles) with a median value of 0.8°C for the EXT green roof (Figure 6b).

Huge differences occurred between surface temperature of the REF, EXT and SI roofs at the daily scale (Figure 2c). The surface temperatures for both the EXT and SI green roofs exhibited a similar daily evolution, following the same dynamics than the REF roof: they increased during the morning to reach their maximum around noon before decreasing during the afternoon to their minimum and nocturnal value. However, maximum mean half-hourly surface temperatures only peaked to 8.4°C and 8.9°C for the EXT and SI green roofs, respectively, while it reached 13°C for the REF roof. The nocturnal surface temperatures are similar between the EXT and REF roofs, around 3.5-5°C, but the SI green roof exhibited systematic slightly warmer surface, around 4.5-6°C (Figure 2c).

Overall, EXT and SI green roofs only had a slight negative (i.e., cooling) effect on winter surface urban heat island as reported by Teemusk and Mander [40]. However, under diurnal conditions the presence of green roofs resulted in surface cooling. Although this cooling for the SI green roof could be due its higher albedo compared to the REF roof, it would not be consistent for the EXT green roof (its albedo being lower than those of the REF roof, warmer surface would be expected). Hence, it would be probably due to low but significant evapotranspiration even during winter conditions [39,44], which is comparable for EXT and SI green roofs according to Silva et al. [44]. Nevertheless, the SI green roof exhibited systematically warmer surface temperature, by around 1°C, inducing that it had a positive (i.e., warming) effect during the nocturnal conditions compared to the REF roof. It is probably due to its thicker substrate allowing a larger heat capacity and thermal inertia and therefore a slower surface cooling during nighttime.

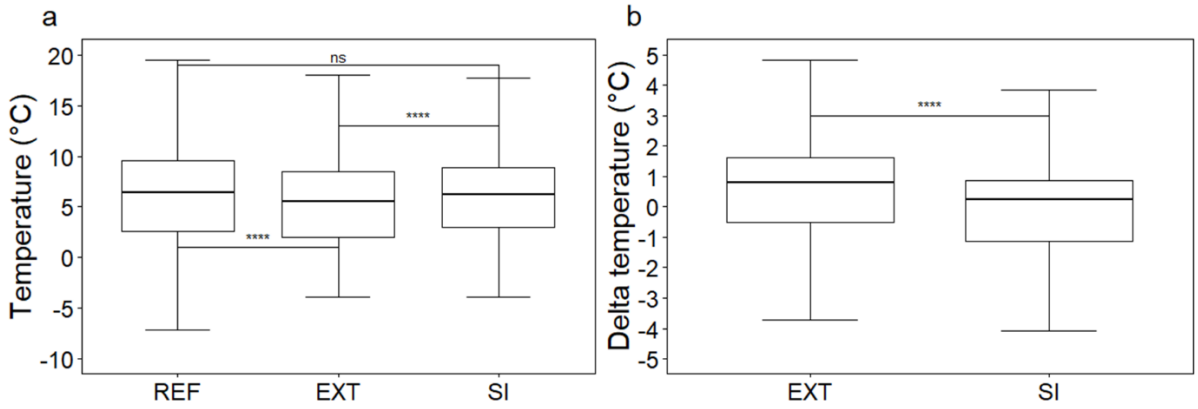


**Figure 6:** Boxplot statistics of **(a)** the surface temperatures of the reference (REF), extensive (EXT), and semi-intensive (SI) roofs, and **(b)** the half-hourly differences between surface temperature of the reference roof and the surface temperature for the green roofs. Are also indicated the results from the Wilcoxon statistical test (ns = p-value > 0.05, **** = p-value < 0.0001).

## 4 –CONCLUSIONS

This study attempted to investigate the impact of two kinds of green roofs i.e., extensive (EXT) and semi-intensive (SI) green roofs, on both building insulation and surface urban heat island effect under winter conditions. To this aim we compared measurements of surface and building envelope temperatures as well as conductive heat fluxes reaching the external building envelope with those measured on a conventional bituminous roof under identical climatic conditions.

While the SI green roof provides a building envelope surface warming compared to the conventional bituminous roof, the EXT green roof has no clear effect on average. However, at the daily scale, although the conventional roof benefits to diurnal solar radiation, and therefore surface heating, it is also exposed to important radiative heat losses during nighttime. On the contrary, green roofs provide an additional insulation layer which diminishes the daily fluctuations of building envelope temperature under winter conditions whatever the kind of green roof. As a consequence, the conductive heat fluxes reaching the external building envelope also suffer to more daily fluctuations for the conventional bituminous roof than for the green roofs. These effects are all the more important that the substrate is thick, owing to its larger heat capacity and thermal inertia. Although it has not been quantified, it could be hypothesized that the reduction of daily fluctuations of conductive heat fluxes would also reduce the building energy consumption by reducing heating loads.

On average the green roofs only have an insignificant or slight effect on surface UHI. However they provide a surface cooling during daytime due to even low but significant evapotranspiration. During nighttime the EXT green roof exhibits similar surface temperature than the conventional roof, while the SI green roof is warmer.

Therefore green roofs can be suitable urban greening solutions since they do not have negative effect on surface urban heat island during winter while they provide an efficient cooling under summer conditions, and provide building insulation [24,28,31,33].

**Acknowledgements**

This work was supported by a grant from Vinci Construction France. The authors also acknowledge Hacene Bouhoun-Ali for its help in the experimental set-up and data acquisition.

**Declaration of interest**

The authors declare that they have no known competing financial interests or personal relationships that could have appeared to influence the work reported in this paper.

**References**

[1] IPCC, 2014: Climate Change 2014: Mitigation of Climate Change. Contribution of Working Group III to the Fifth Assessment Report of the Intergovernmental Panel on Climate Change [Edenhofer, O., R. Pichs-Madruga, Y. Sokona, E. Farahani, S. Kadner, K. Seyboth, A. Adler, I. Baum, S. Brunner, P. Eickemeier, B. Kriemann, J. Savolainen, S. Schlömer, C. von Stechow, T. Zwickel and J.C. Minx (eds.)]. Cambridge University Press, Cambridge, United Kingdom and New York, NY, USA.

[2] W.G.V. Balchin, N. Pye, A micro-climatological investigation of Bath and the surrounding district, Q. J. Roy. Meteor. Soc. 73 (1947) 297-323.

[3] T.R. Oke, The energetic basis of the urban heat island, Q. J. Roy. Meteor. Soc. 108 (1982) 1-24.

[4] H. Akbari, M. Pomerantz, H. Taha, Cool surfaces and shade trees to reduce energy use and improve air quality in urban areas, Sol. Energy. 70 (2001) 295-310.

[5] C. Li, J. Zhou, Y. Cao, J. Zhong, Y. Liu, C. Kang, Y. Tan, Interaction between urban microclimate and electric air-conditioning energy consumption during high temperature season, Appl. Energ. 117 (2014) 149-156.

[6] S. Vandentorren, F. Suzan, S. Medina, M. Pascal, A. Maulpoix, J.C. Cohen, M. Ledrans, Mortality in 13 French cities during the August 2003 heat wave, Am. J. Public. Health. 94 (2004) 1518-1520.

[7] M. Duneier, Ethnography, the ecological fallacy, and the 1995 Chicago heat wave, Am. Sociol. Rev. 71 (2006) 679-688.

[8] S.L. Harlan, D.M. Ruddell, Climate change and health in cities: impacts of heat and air pollution and potential co-benefits from mitigation and adaptation, Curr. Opin. Env. Sust. 3 (2011) 126-134.

[9] A.H. Rosenfeld, H. Akbari, J.J. Romm, Cool communities: Strategies for heat island mitigation and smog reduction, Energ. Buildings. 28 (1998) 51-62.

[10] C. Sarrat, A. Lemonsu, V. Masson, D. Guedalia, Impact of urban heat island on regional atmospheric pollution, Atmos. Environ. 40 (2006) 1743-1758.

[11] G. Pigeon, D. Legain, P. Durand, V. Masson, Anthropogenic heat release in an old European agglomeration (Toulouse, France), Int. J. Climatol. 27 (2007) 1969-1981.

[12] Y. Wen, Z. Lian, Influence of air conditioners utilization on urban thermal environment, Appl. Therm. Eng. 29 (2009) 670-675.

[13] C. de Munck, G. Pigeon, V. Masson, F. Meunier, P. Bousquet, B. Tréméac, M. Merchat, P. Poeuf, C. Marchadier, How much can air conditioning increase air temperatures for a city like Paris, France?, Int. J. Climatol. 33 (2013) 210-227.

[14] F. Asdrubali, F. D'Alessandro, S. Schiavoni, A review of unconventional sustainable building insulation materials, Sustain. Mater. Technol. 4 (2015) 1-17.

[15] S. Schiavoni, F. D'Alessandro, F. Bianchi, F. Asdrubali, Insulation materials for the building sector: A review and comparative analysis, Renew. Sust. Energ. Rev. 62 (2016) 988-1011.

[16] D. Prakash, A review of heat dissipating passive cooling techniques for residential buildings at tropical region, J. Eng. Sci. Technol. 8 (2012) 2120-2140.

[17] N. Mirabella, M. Röck, M.R.M. Saade, C. Spirinckx, M. Bosmans, K. Allacker, A. Passer, Strategies to improve the energy performance of buildings: a review of their life cycle impact, Buildings 8 (2018) 105. doi:10.3390/buildings8080105.

[18] J. Yang, Q. Yu, P. Gong, Quantifying air pollution removal by green roofs in Chicago, Atmos. Environ. 42 (2008) 7266-7273.

[19] Y. Li, R.W. Babcock Jr., Green roofs against pollution and climate change. A review. Agron. Sustain. Dev. 34 (2014) 695-705.

[20] N. Dunnett, A. Nagase, R. Booth, P. Grime, Influence of vegetation composition on runoff in two simulated green roof experiments, Urban Ecosyst. 11 (2008) 385-398.

[21] E. Cristiano, R. Deidda, F. Viola, The role of green roofs in urban Water-Energy-Food-Ecosystem nexus: A review. Sci. Tot. Environ. 756 (2021) 143876.

[22] U. Berardi, A.H. GhaffarianHoseini, A. GhaffarianHoseini, State-of-the-art analysis of the environmental benefits of green roofs, Appl. Energ. 115 (2014) 411-428.

[23] L.L. Peng, C.Y. Jim, Green-roof effects on neighborhood microclimate and human thermal sensation, Energies 6 (2013) 598–618.

[24] C. de Munck, A. Lemonsu, V. Masson, J. Le Bras, M. Bonhomme, Evaluating the impacts of greening scenarios on thermal comfort and energy and water consumptions for adapting Paris city to climate change, Urban Climatol. 23 (2018) 260–286.

[25] B. Raji, M.J. Tenpierik, A. van den Dobbelsteen, The impact of greening systems on building energy performance: A literature review, Renew. Sust. Energ. Rev. 45 (2015) 610-623.

[26] A. Niachou, K. Papakonstantinou, M. Santamouris, A. Tsangrassoulis, G. Mihalakakou, Analysis of the green roof thermal properties and investigation of its energy performance, Energ. Buildings 33 (2001) 719-729.

[27] N. Wong, Y. Chen, C. Ong, A. Sia, Investigation of thermal benefits of rooftop garden in the tropical environment, Build. Environ. 38 (2003) 261–270.

[28] I. Jaffal, S.E. Ouldboukhitine, R. Belarbi, A comprehensive study of the impact of green roofs on building energy performance, Renew. Energ. 43 (2012) 157–164.

[29] L.M. Cook, T.A. Larsen, Towards a performance-based approach for multifunctional green roofs: An interdisciplinary review, Build. Environ. 188 (2021) 107489.

[30] M. Maiolo, B. Pirouz, R. Bruno, S.A. Palermo, N. Arcuri, P. Piro, The role of the extensive green roofs on decreasing building energy consumption in the Mediterranean climate, Sustainability 12 (2020) 359.

[31] R. Kumar, S.C. Kaushik, Performance evaluation of green roof and shading for thermal protection of buildings, Build. Environ. 40 (2005) 1505–1511.

[32] H.F. Castleton, V. Stovin, S.B.M. Beck, J.B. Davison, Green roofs, building energy savings and the potential for retrofit, Energ. Buildings 42 (2010) 1582-1591.

[33] G. Qiu, H. Li, Q. Zhang, W. Chen, X. Liang, X. Li, Effects of evapotranspiration on mitigation of urban temperature by vegetation and urban agriculture, J. Integr. Agr. 12 (2013) 1307–1315.

[34] M. Eksi, D.B. Rowe, I.S. Wichman, J.A. Andresen, Effect of substrate depth, vegetation type, and season on green roof thermal properties, Energ. Buildings 145 (2017) 174–187.

[35] Y. Yang, C.I. Davidson, J. Zhang, Evaluation of thermal performance of green roofs via field measurements and hygrothermal simulations, Energ. Buildings 237 (2021) 110800.

[36] M. Santamouris, C. Pavlou, P. Doukas, G. Mihalakakou, A. Synnefa, A. Hatzibiros, P. Patargias, Investigating and analysing the energy and environmental performance of an experimental green roof system installed in a nursery school building in Athens, Greece, Energy 32 (2007) 1781–1788.

[37] J. Coma, G. Pérez, C. Solé, A. Castell, L.F. Cabeza, Thermal assessment of extensive green roofs as passive tool for energy savings in buildings, Renew. Energ. 85 (2016) 1106-1115.

[38] J.T. Lundholm, B.M. Weddle, J.S. MacIvor, Snow depth and vegetation type affect green roof thermal performance in winter, Energ. Buildings 84 (2014) 299-307.

[39] R.M. Lazzarin, F. Castellotti, F. Busato, Experimental measurements and numerical modelling of a green roof, Energ. Buildings 37 (2005) 1260-1267.

[40] A. Teemusk, Ü. Mander, Greenroof potential to reduce temperature fluctuations of a roof membrane: A case study from Estonia, Build. Environ. 44 (2009) 643-650.

[41] K.L. Getter, D.B. Rowe, J.A. Andresen, I.S. Wichman, Seasonal heat flux properties of an extensive green roof in Midwestern U.S. climate, Energ. Buildings 43 (2011) 3548-3557.

[42] M. D'Orazio, C. Di Perna, E. Di Giuseppe, Green roof yearly performance: A case study in a highly insulated building under temperate climate, Energ. Buildings 55 (2012) 439-451.

[43] M. Zhao, J. Srebric, Assessment of a green roof performance for sustainable buildings under winter weather conditions, J. Cent. South Univ. 19 (2012) 639-644.

[44] C.M. Silva, M.G. Gomes, M. Silva, Green roofs energy performance in Mediterranean climate, Energ. Buildings 116 (2016) 318-325.

[45] M. Squier, C.I. Davidson, Heat flux and seasonal thermal performance of an extensive green roof, Build. Environ. 107 (2016) 235-244.

[46] S. Collins, K. Kuoppamäki, D.J. Kotze, X. Lü, Thermal behavior of green roofs under Nordic winter conditions, Build. Environ. 122 (2017) 206-214.

[47] H. Radhi, E. Assem, S. Sharples, On the colours and properties of building surface materials to mitigate urban heat islands in highly productive solar regions, Build. Environ. 72 (2014) 162–172.

[48] O. Saadatian, K. Sopian, E. Salleh, C.H. Lim, S. Riffat, E. Saadatian, A. Toudeshki, M.Y Sulaiman, A review of energy aspects of green roofs. Renew. Sust. Energ. Rev. 23 (2013) 155–168.

[49] H. Takebayashi, M. Moriyama, Surface heat budget on green roof and high reflection roof for mitigation of urban heat island. Build. Environ. 42 (2007) 2971–2979.

[50] P.A. Fokaides, S.A. Kalogirou, Application of infrared thermography for the determination of the overall heat transfer coefficient (U-value) in building envelopes. Applied Energ. 88 (2011) 4358-4365.

[51] J.A. Nelson, O. Pérez-Priego, S. Zhou, R. Poyatos, Y. Zhang, P.D. Blanken, T.E. Gimeno, G. Wohlfahrt, A.R. Desai, B. Gioli, J.M. Limousin, D. Bonal, E. Paul-Limoges, R.L. Scott, A. Varlagin, K. Fuchs, L. Montagnani, S. Wolf, N. Delpierre, D. Berveiller, M. Gharun, L. Belilli Marchesini, D. Gianelle, L. Sigut, I. Mammarella, L. Siebicke, T.A. Black, A. Knohl, L. Hörtnagl, V. Magliulo, S. Besnard, U. Weber, N. Carvalhais, M. Migliavacca, M. Reichstein, M. Jung, Ecosystem transpiration and evaporation: Insights from three water flux partitioning methods across FLUXNET sites. Glob. Change Biol. 26 (2020) 6916-6930.